

Supplementary Materials for
**Neuronal correlates of selective attention and effort in visual area V4 are
invariant of motivational context**

Supriya Ghosh and John H. R. Maunsell

Corresponding author: Supriya Ghosh, sghosh5@uchicago.edu

Sci. Adv. **8**, eabc8812 (2022)
DOI: 10.1126/sciadv.abc8812

The PDF file includes:

Figs. S1 to S16
Tables S1 to S4
Legends for data S1 to S3

Other Supplementary Material for this manuscript includes the following:

Data S1 to S3

Table S1. Behavioral d' controlled by differential task difficulty

Monkey S (Sessions, N = 20)	d'_{inRF} (Mean \pm SEM)	d'_{oppRF} (Mean \pm SEM)	Selectivity index (Mean \pm SEM)	Effort (Mean \pm SEM)
Low selective inRF	0.96 ± 0.04	2.79 ± 0.07	-0.58 ± 0.01	2.96 ± 0.07
High selective inRF	2.64 ± 0.06	1.03 ± 0.03	0.52 ± 0.01	2.84 ± 0.06
Non-selective low effort	0.98 ± 0.04	1.07 ± 0.03	-0.05 ± 0.02	1.46 ± 0.04
Non-selective high effort	2.63 ± 0.06	2.78 ± 0.06	-0.04 ± 0.01	3.84 ± 0.08

Monkey P (Sessions, N = 22)	d'_{inRF} (Mean \pm SEM)	d'_{oppRF} (Mean \pm SEM)	Selectivity index (Mean \pm SEM)	Effort (Mean \pm SEM)
Low selective inRF	1.28 ± 0.06	2.53 ± 0.08	-0.41 ± 0.02	2.84 ± 0.09
High selective inRF	2.85 ± 0.08	1.29 ± 0.05	0.46 ± 0.01	3.14 ± 0.09
Non-selective low effort	1.20 ± 0.05	1.20 ± 0.06	0.01 ± 0.02	1.71 ± 0.07
Non-selective high effort	2.71 ± 0.08	2.62 ± 0.1	0.02 ± 0.02	3.78 ± 0.11

Table S2. Behavioral d' controlled by differential reward size

Monkey S (Sessions, N = 20)	d'_{inRF} (Mean \pm SEM)	d'_{oppRF} (Mean \pm SEM)	Selectivity index (Mean \pm SEM)	Effort (Mean \pm SEM)
Low selective inRF	0.79 \pm 0.05	2.73 \pm 0.07	-0.64 \pm 0.02	2.84 \pm 0.08
High selective inRF	2.61 \pm 0.08	0.98 \pm 0.06	0.54 \pm 0.02	2.80 \pm 0.08
Non-selective low effort	0.99 \pm 0.03	1.05 \pm 0.04	-0.04 \pm 0.02	1.45 \pm 0.05
Non-selective high effort	2.53 \pm 0.08	2.72 \pm 0.07	-0.05 \pm 0.01	3.72 \pm 0.1

Monkey P (Sessions, N = 16)	d'_{inRF} (Mean \pm SEM)	d'_{oppRF} (Mean \pm SEM)	Selectivity index (Mean \pm SEM)	Effort (Mean \pm SEM)
Low selective inRF	1.10 \pm 0.05	2.51 \pm 0.05	-0.47 \pm 0.02	2.75 \pm 0.05
High selective inRF	2.66 \pm 0.05	1.15 \pm 0.05	0.48 \pm 0.02	2.91 \pm 0.06
Non-selective low effort	1.05 \pm 0.06	1.11 \pm 0.06	-0.04 \pm 0.03	1.53 \pm 0.07
Non-selective high effort	2.68 \pm 0.07	2.54 \pm 0.08	0.04 \pm 0.02	3.70 \pm 0.09

Table S3. Behavioral criterion in task difficulty manipulation sessions

Monkey S (Sessions, N = 20)	Criterion _{inRF}		Criterion _{oppRF}	
	Mean	95% CI	Mean	95% CI
Low selective inRF	-0.03	[-0.09, 0.02]	-0.15	[-0.23, -0.06]
High selective inRF	-0.33	[-0.41, -0.25]	-0.05	[-0.11, 0.01]
Non-selective low effort	-0.22	[-0.28, -0.16]	-0.20	[-0.25, -0.15]
Non-selective high effort	-0.29	[-0.39, -0.17]	-0.01	[-0.12, 0.10]

Monkey P (Sessions, N = 22)	Criterion _{inRF}		Criterion _{oppRF}	
	Mean	95% CI	Mean	95% CI
Low selective inRF	-0.04	[-0.18, 0.10]	-0.73	[-0.82, -0.63]
High selective inRF	-0.39	[-0.47, -0.32]	-0.03	[-0.13, 0.06]
Non-selective low effort	-0.14	[-0.22, -0.06]	-0.15	[-0.23, -0.07]
Non-selective high effort	-0.28	[-0.39, -0.17]	-0.39	[-0.47, -0.31]

Table S4. Behavioral criterion in reward manipulation sessions

Monkey S (Sessions, N = 16)	Criterion _{inRF}		Criterion _{oppRF}	
	Mean	95% CI	Mean	95% CI
Low selective inRF	-0.09	[-0.21, 0.02]	-0.38	[-0.49, -0.27]
High selective inRF	-0.17	[-0.26, -0.09]	-0.07	[-0.13, -0.02]
Non-selective low effort	-0.09	[-0.17, -0.01]	-0.11	[-0.21, -0.01]
Non-selective high effort	-0.14	[-0.22, -0.06]	-0.21	[-0.29, -0.14]

Monkey P (Sessions, N = 20)	Criterion _{inRF}		Criterion _{oppRF}	
	Mean	95% CI	Mean	95% CI
Low selective inRF	-0.02	[-0.08, 0.05]	-0.22	[-0.30, -0.13]
High selective inRF	-0.19	[-0.28, -0.1]	-0.03	[-0.05, 0.10]
Non-selective low effort	-0.23	[-0.31, -0.16]	-0.20	[-0.28, -0.12]
Non-selective high effort	-0.22	[-0.30, -0.15]	-0.07	[-0.19, 0.06]

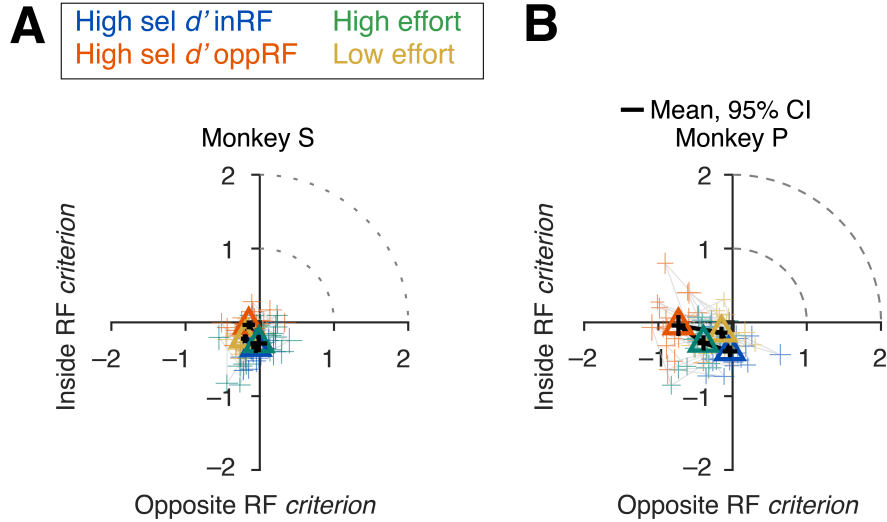


Fig. S1. Behavioral criteria associated with attentional selectivity and effort controlled by task difficulty. (A-B) Attention operating characteristic (AOC) curve, indicating behavioral criterion on individual sessions and their average (triangles) for test stimuli inside and opposite side of the RF during four attention conditions (#sessions: 20 monkey S (A); 22 monkey P (B)). Attention conditions had no significant effect on criteria for monkey S ($F_{(3, 176)} = 2.7$, $P > 0.05$, ANOVA). For monkey P, there was significant effect on criterion by attention conditions ($F_{(3, 171)} = 6.1$, $P < 0.01$, ANOVA). Lines connect four attention conditions within a session. Error bars, 95% confidence intervals).

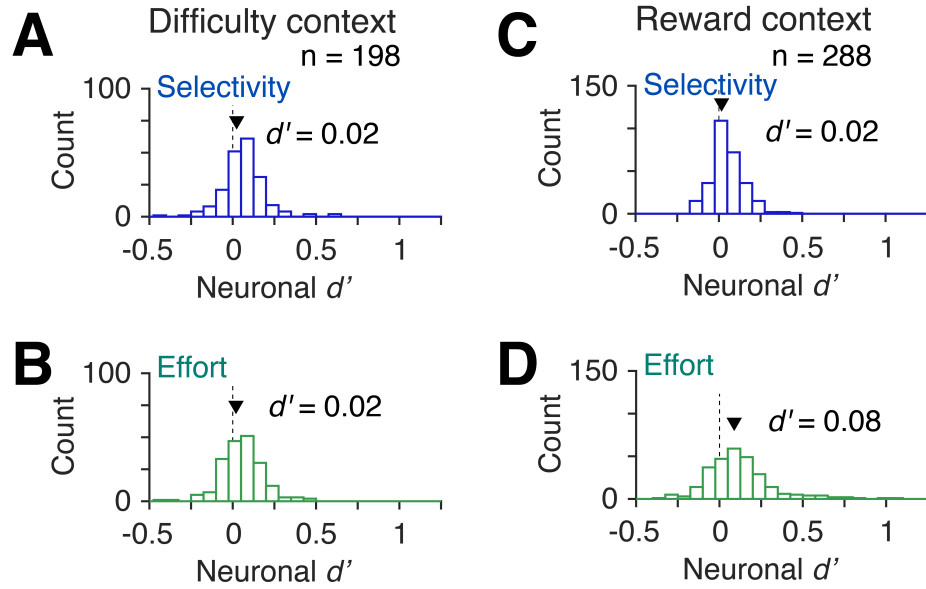


Fig. S2. Neuronal d' based on pre-sample spike counts (–200 to 0 ms) of visually non-responsive units for task difficulty (neurons, $n = 198$) and reward (neurons, $n = 288$) contexts in both monkeys. (A–B) Neuronal d' 's in difficulty sessions for selective attention (mean \pm SEM, $d' = 0.02 \pm 0.01$, $p < 0.05$) (A) and for attentional effort (mean \pm SEM, $d' = 0.02 \pm 0.01$, $p < 0.05$) (B). (C–D) Same as in A and B, but for the reward sessions (mean \pm SEM for selective attention, $d' = 0.02 \pm 0.006$, $p < 0.05$; for attentional effort, $d' = 0.08 \pm 0.013$, $p < 0.05$).

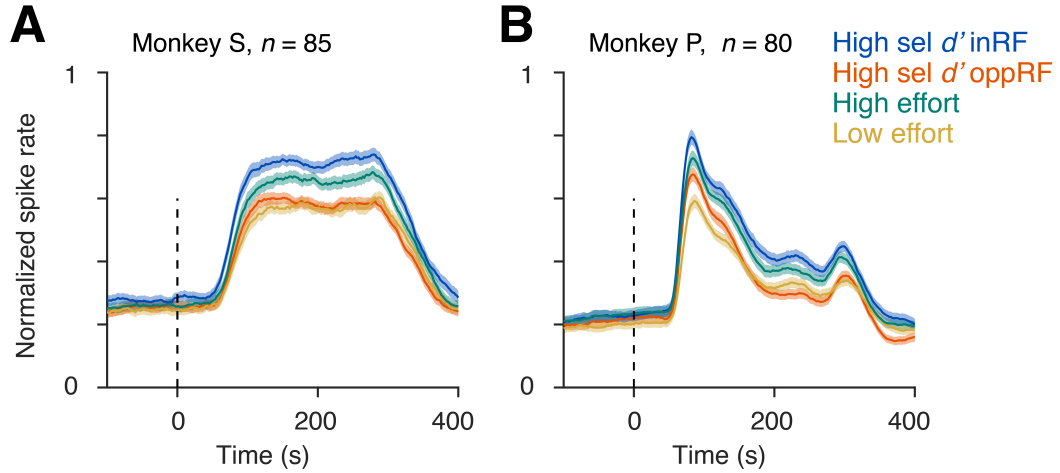


Fig. S3. Peri-stimulus time histograms (PSTH) of unique units across recording sessions. A unique unit was randomly selected from every electrode out of a multielectrode array (96 channel) across session for individual monkeys (monkey S, $n = 85$ (A); monkey P, $n = 80$ (B)). Error bars, mean \pm SEM.

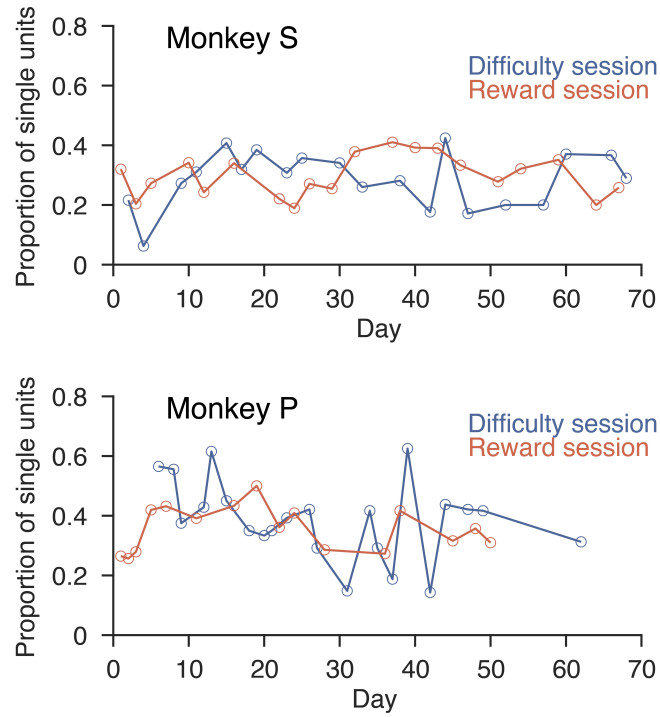


Fig. S4. Proportion of single units across all experimental sessions. Difficulty and reward context sessions were interleaved. The proportions of single units (ratio of the number of single units to total number of units) between the task contexts did not differ for both the monkeys (monkey S: median (inter-quartile range) for task difficulty sessions, 0.30 (IQR 0.21, 0.36); for reward sessions, 0.30 (IQR 0.25, 0.35), $p = 0.78$, rank sum test; monkey P: median (inter-quartile range) for task difficulty session, 0.40 (IQR 0.31, 0.44), for reward session, 0.36 (IQR 0.28, 0.42), $p = 0.29$, rank sum test).

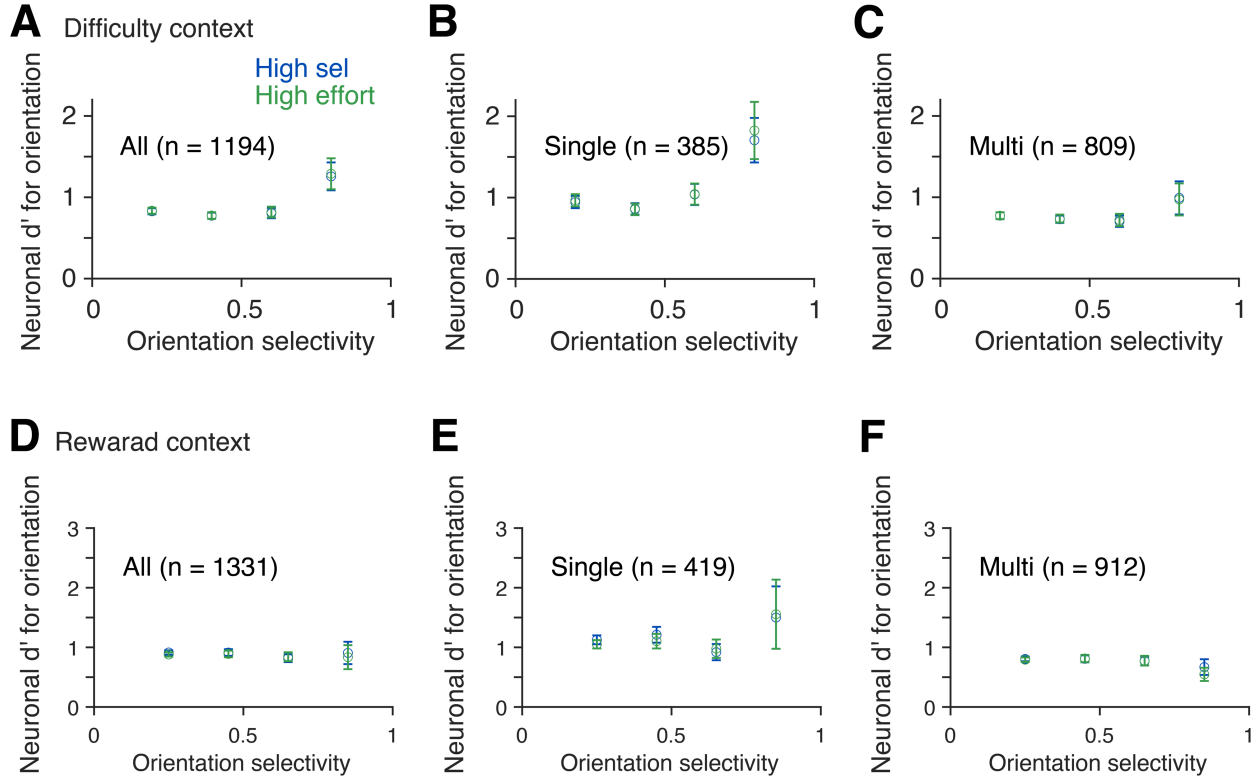
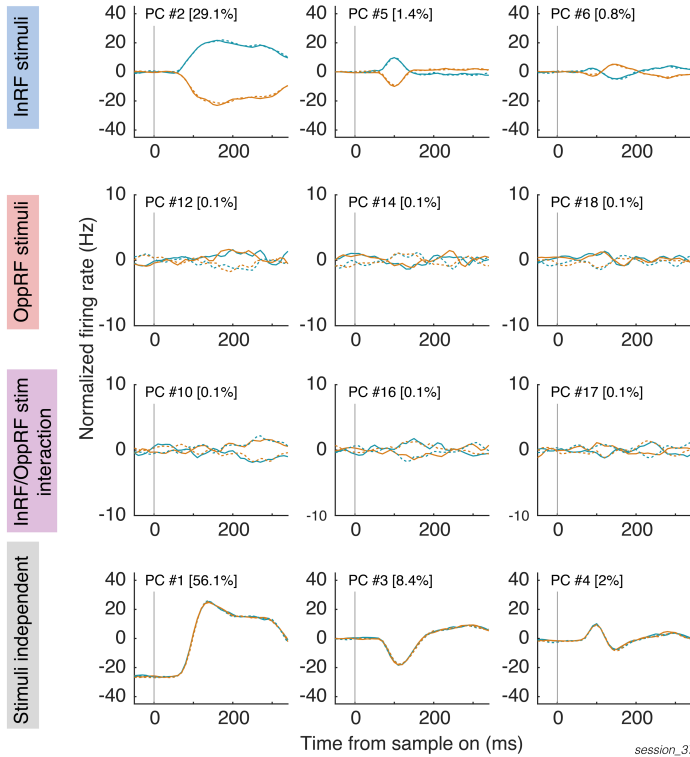


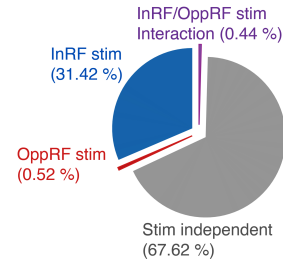
Fig. S5. Neuronal d' for stimulus orientation discrimination. (A-C) Population averaged neuronal d' for stimulus orientation discrimination in the RF location for high inRF selective attention and high effort trial blocks of all units (A), single units (B) and multiunits (C) for the difficulty context. Where, neuronal $d' = [\text{abs}(r_1 - r_2) / \sqrt{(\text{SD}_1^2 + \text{SD}_2^2)/2}]$; r_1 and r_2 are spike counts (60-260 ms from sample onset) for the two stimulus orientations in the RF location; SD_1 and SD_2 are standard deviations of spike counts for the two orientations. Units were grouped according to their orientation selectivity. Orientation selectivity = $(1/\sigma - 1/\sigma_{\max}) * \sigma_{\min}$. It scales between 0 (no selectivity) and 1 (highly selective). Where, σ corresponds to the width of the orientation tuning curve. σ_{\max} and σ_{\min} are respectively the maxima and minima of the widths of the orientation tuning curve. (D-F) Same as in (A-C) except for varying reward context sessions.

A Example session (High inRF sel. attention)

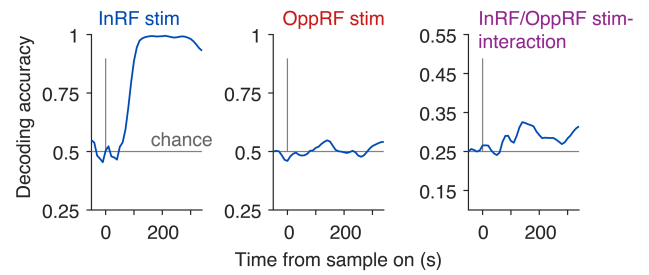
— InRF ori 1 - - - OppRF ori 1
— InRF ori 2 - - - OppRF ori 2



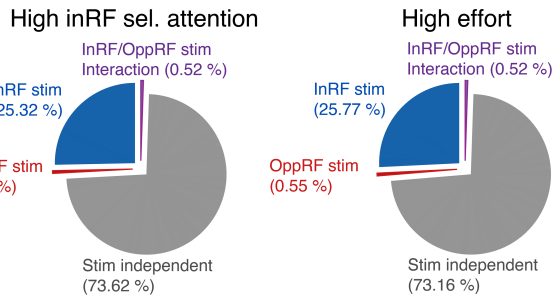
B Example session



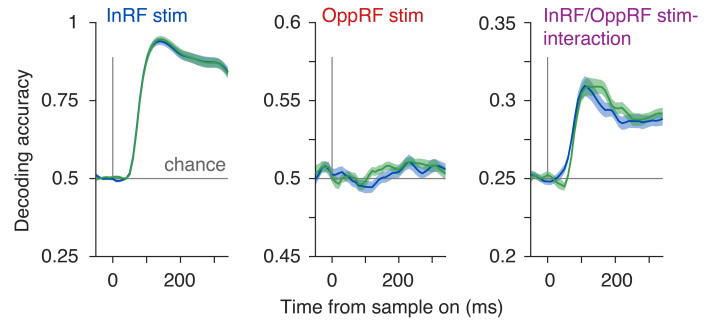
C Example session Mean \pm sem



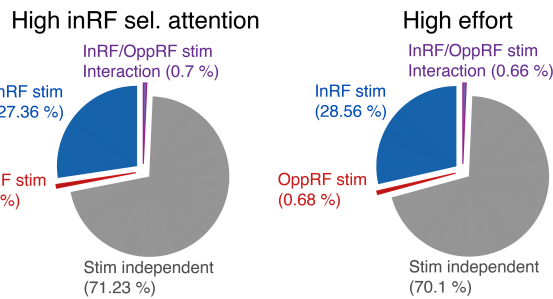
D Population: Difficulty sessions (N = 42)



E Population: Difficulty sessions (N = 42) Mean \pm sem



F Population: Reward sessions (N = 36)



G Population: Reward sessions (N = 36) Mean \pm sem

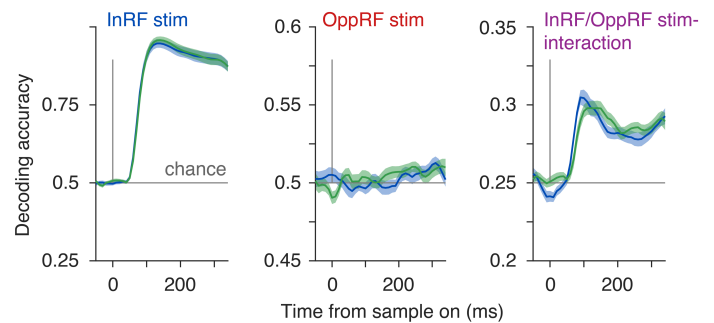


Fig. S6. Information content of stimulus orientation estimated using demixed principal components. Spike rates of simultaneously recorded population of neurons within each session are decomposed into few components by systematically capturing most of the variance of the data with taking into account of stimulus/experimental conditions [Kobak *D et. al.*, *eLife*, 2016 (27)]. Each of these components (demixed principal component) carries information of a single aspect of the task condition (stimulus/experimental). Information about stimulus orientation at the two locations in opposite visual hemifields have been isolated from the rest of the task variables. Trials were classified into 2 stimulus conditions: according to the Gabor orientation in the RF location (two orientations: $\text{base}_{\text{inRF}}$ and $\text{base}_{\text{inRF}} + 90^\circ$) and in the opposite RF location (two orientations: $\text{base}_{\text{oppRF}}$ and $\text{base}_{\text{oppRF}} + 90^\circ$) during the sample period. Thus, there were total 4 different configurations of stimulus orientation. Single-trial spike rates were filtered with a half Gaussian kernel ($\sigma = 50$ ms) and subsamples at 100 Hz. Spike rates over 400 ms (40 time points) starting from -50 ms to 350 ms from the sample stimulus onset were used for the analysis (Materials and Methods). (A) Demixed principal components were arranged according to the stimulus conditions in an example session. Explained variances of the components are shown as percentages. Traces in each subplot are the projections of PSTH data onto the respective demixed principal component decoder axis and correspond to 4 stimulus conditions. *Top row*, first three components for stimulus orientation in the RF location. *Second row*, first three components for stimulus orientation in the opposite RF location. *Third row*, first three components for the interaction between the inRF and oppRF stimuli. *Fourth row*, stimulus independent components. (B) Total explained variance of the individual demixed principal components for the same example session as in (A). (C) Cross-validated (leave-one-out; repetitions, $n = 1000$) classification accuracies for linear classifiers using the first three demixed principal components associated with each stimulus condition to discriminate stimulus orientations in the RF location (*left*), opposite RF location (*middle*) and combined stimuli (*right*) for the same example session as in (A). (D) Session averaged total explained variances for the trials during high selective attention in the RF location (*left*) and high effort (*right*) in difficulty sessions from the two monkeys ($N = 42$). (E) Session averaged cross-validated classification accuracies in difficulty sessions ($N = 42$) for high selective attention and high effort same as in (C). (F-G) Same as in (D) and (F), but for reward sessions from both the monkeys ($N = 36$). [Reference: Kobak, D. *et al.* Demixed principal component analysis of neural population data. *Elife* 5, e10989 (2016) (27).]

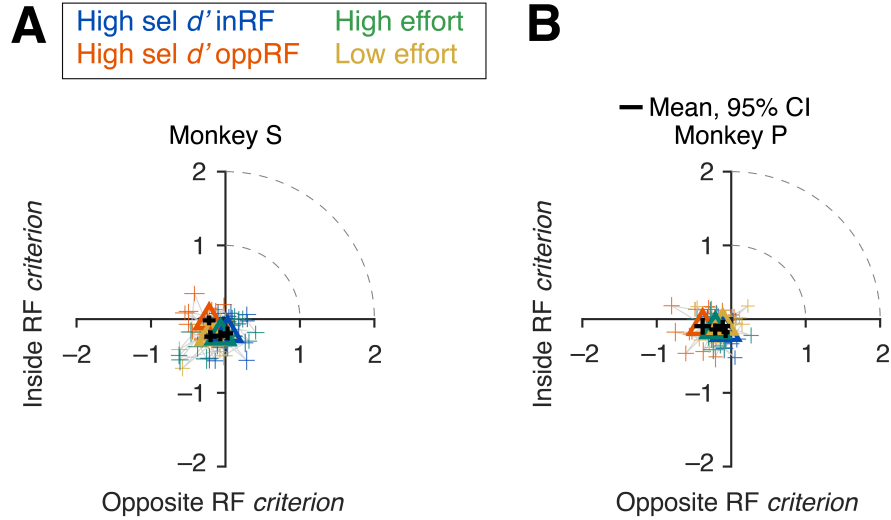


Fig. S7. Behavioral criteria associated with attentional selectivity and effort controlled by reward size. (A-B) Attention operating characteristic (AOC) curve, indicating behavioral criterion on individual sessions and their average (triangles) for test stimuli inside and opposite side of the RF during four attention conditions (sessions, $N = 20$, monkey S (A); $N = 16$, monkey P (B)). Attention conditions had significant effect on criteria in monkey S ($F_{(3, 155)} = 2.96$, $P < 0.05$, ANOVA) and monkey P ($F_{(3, 123)} = 3.14$, $P < 0.01$, ANOVA). Lines connect four attention conditions within a session. Error bars, 95% confidence intervals.

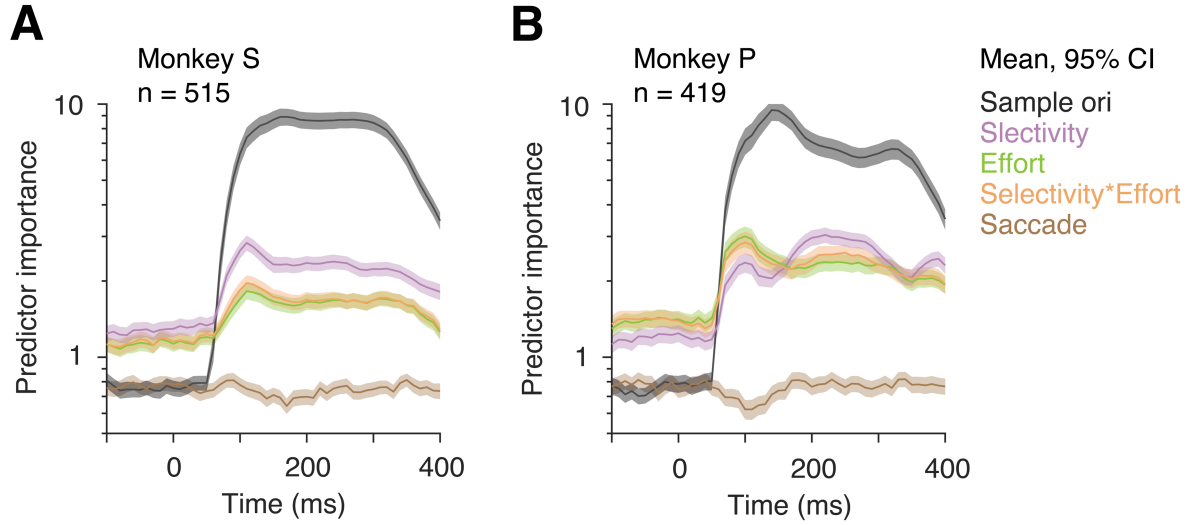


Fig. S8. Encoding of attention components within single-trial spike trains in task-difficulty context. (A-B) Comparing predictor importance (PI) that measures contributions of different predictor variables estimated by absolute standardized predictor coefficient values of recorded units from monkey S (A, units, $n = 515$) and monkey P (B, units, $n = 419$) that were significant fit with the generalized linear model in **Fig. 5E**. Error bars, 95% confidence intervals (bootstrap, $n = 10^4$).

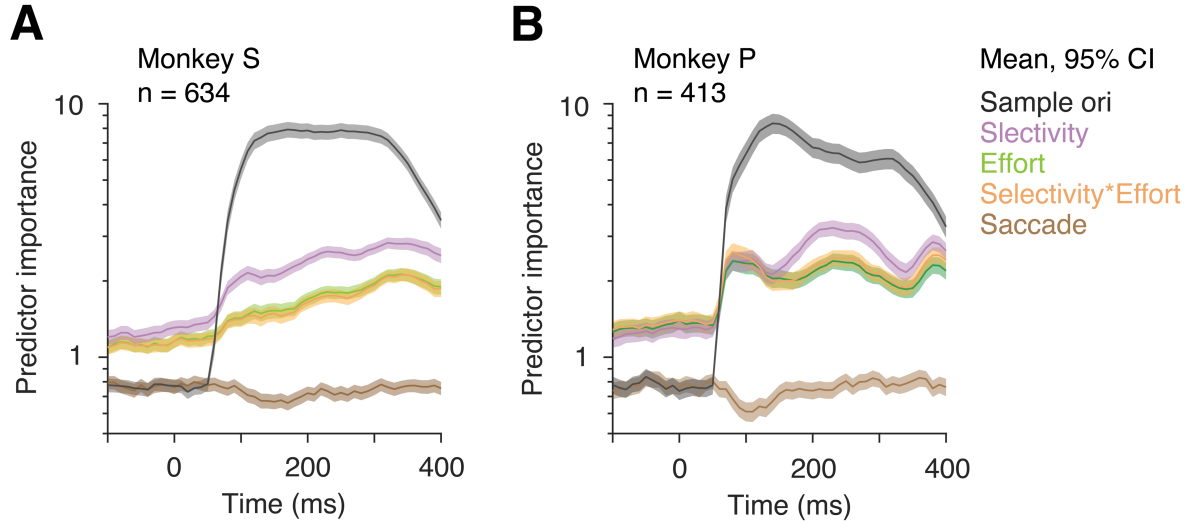


Fig. S9. Encoding of attention components within single-trial spike trains in reward context sessions. (A-B) Comparing predictor importance (PI) that measures contributions of different predictor variables estimated by absolute standardized predictor coefficient values of recorded units from monkey S (A, n = 634) and monkey P (B, n = 413) that were significant fit with the generalized linear model in **Fig. 5G**. Error bars, 95% confidence intervals (bootstrap, n = 10^4).

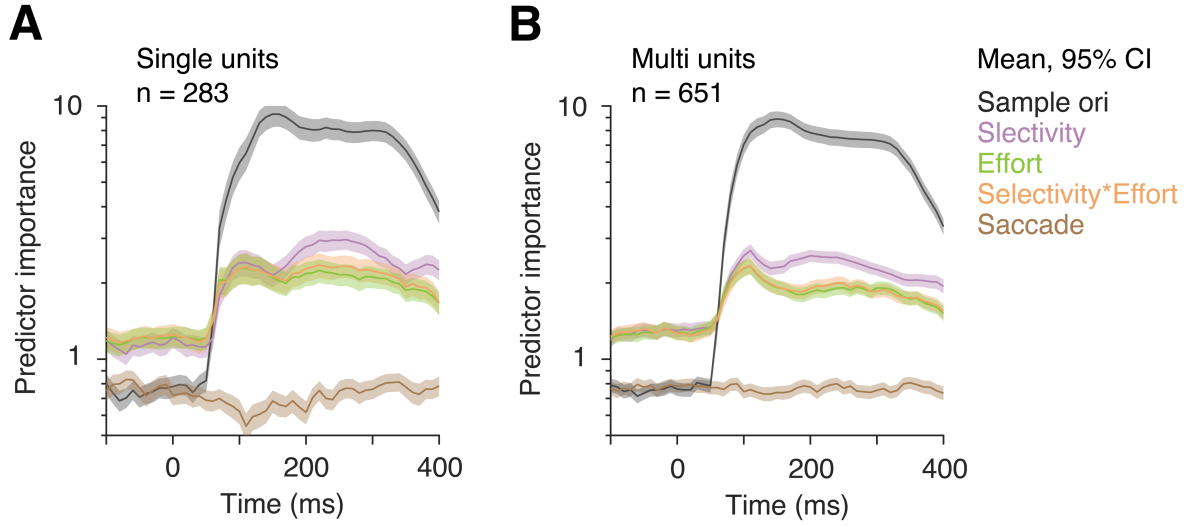


Fig. S10. Predictor importance for single- and multi-units in task-difficulty context. Comparing predictor importance that measures contributions of different predictor variables estimated by absolute standardized predictor coefficient values of all well fitted single (A) and multi units (B). Error bars, 95% confidence intervals (bootstrap, $n = 10^4$).

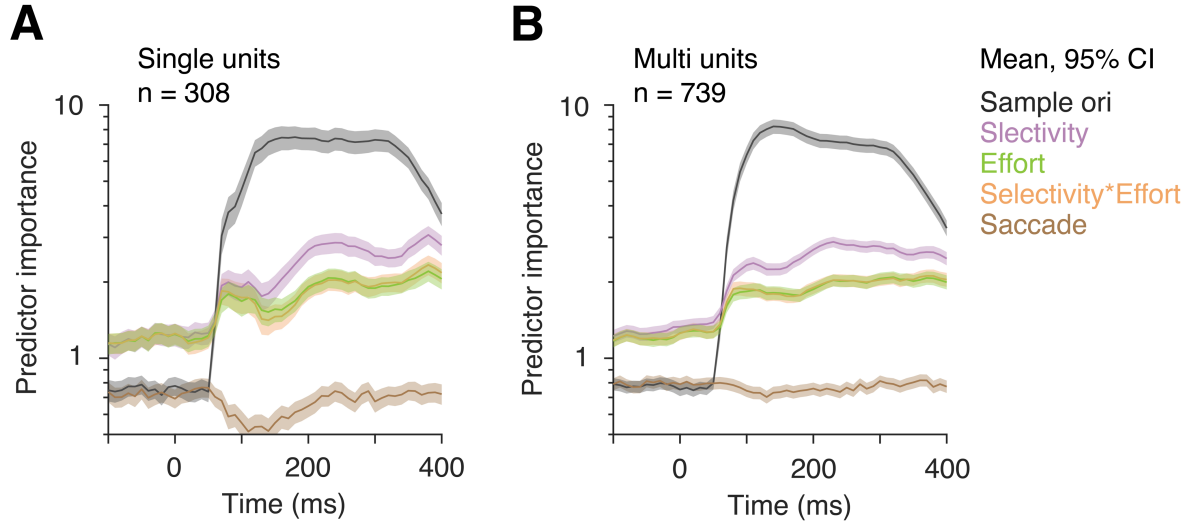


Fig. S11. Predictor importance for single- and multi-units in reward context sessions. Comparing predictor importance that measures contributions of different predictor variables estimated by absolute standardized predictor coefficient values of all well fitted single- (A) and multi-units (B). Error bars, 95% confidence intervals (bootstrap, $n = 10^4$).

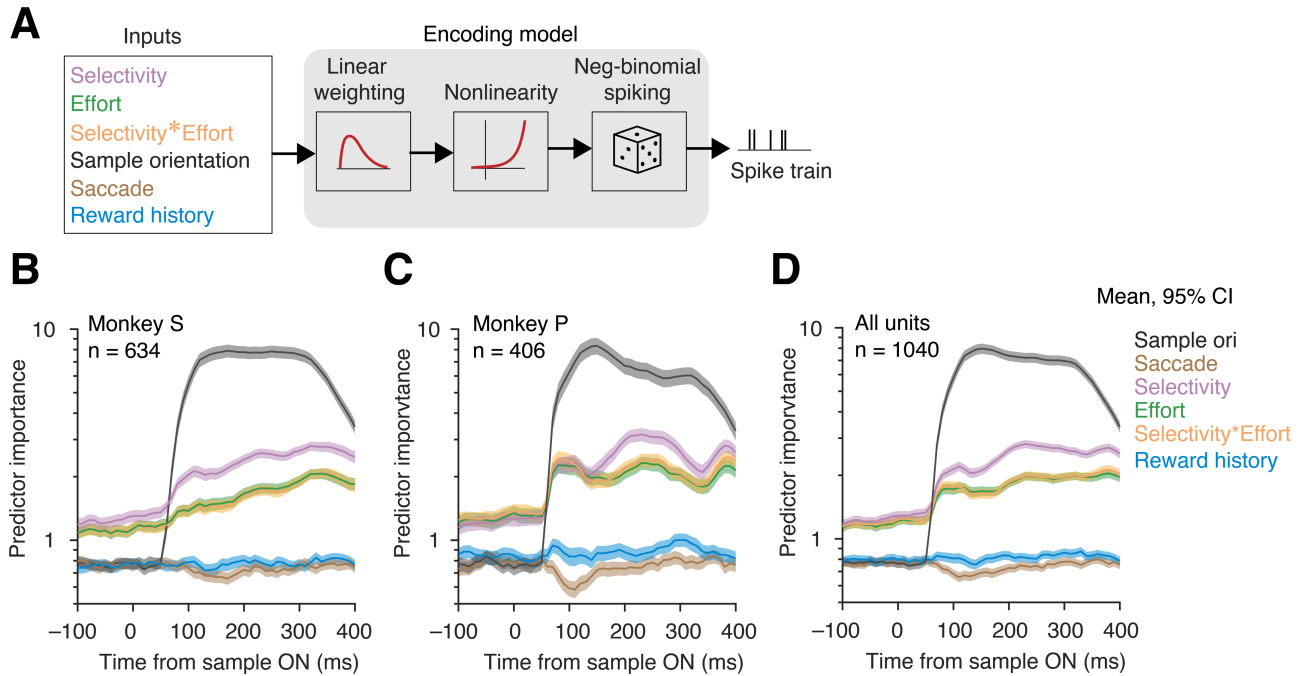


Fig. S12. Alternate encoding model containing reward history: reward context sessions. (A) An alternate generalized linear encoding model with reward history as an additional variable. A neuron's spike count over 50 ms sliding window (10 ms shift) is modeled as exponential function of linear combination of weighted (β coefficient) experimental variables: stimulus orientation, reward history (average of received rewards in 3 immediate past trials), saccade, attentional selectivity, attentional effort and their interaction selectivity*effort. (B-D) Comparing predictor importance (PI) that measures contributions of different predictor variables estimated by absolute standardized predictor coefficient values of recorded units from monkey S (B, n = 634) and monkey P (C, n = 413) and both monkeys (D, n = 1040) that were significant fit with the generalized linear model. Error bars, 95% confidence intervals (bootstrap, n = 10^4).

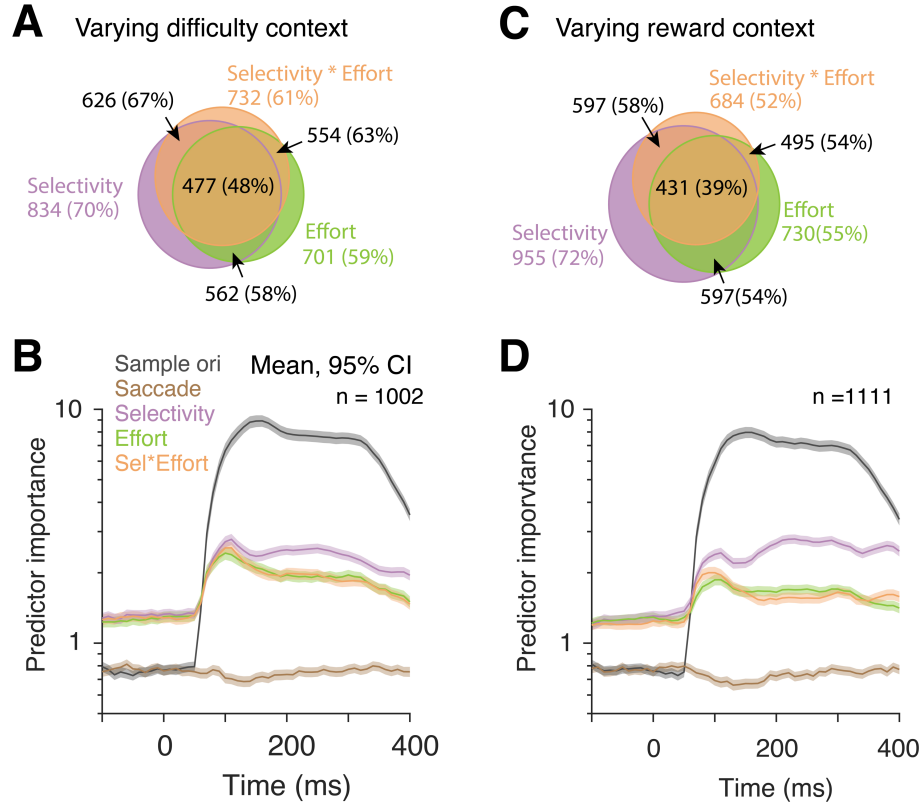


Fig. S13. Single trial encoding of attention components in different motivation contexts. (A-B) Varying task-difficulty context. Proportion of neurons that are modulated ($p < 0.05$) by attentional selectivity, effort and selectivity-by-effort interaction (A) estimated from the model in **Fig. 5A**. Selectivity was represented by the selectivity index $[(4/\pi) \cdot \tan^{-1}(d'_{\text{inRF}}/d'_{\text{oppRF}}) - 1]$. Comparing predictor importance (PI) that measures contributions of different predictor variables estimated by absolute standardized predictor coefficient values of all well fitted neurons (B). Error bars, 95% confidence intervals (bootstrap, $n = 10^4$). **(C-D)** Varying reward context. Same as (A) and (B) when attention was controlled by differential reward sizes. Error bars, 95% confidence intervals.

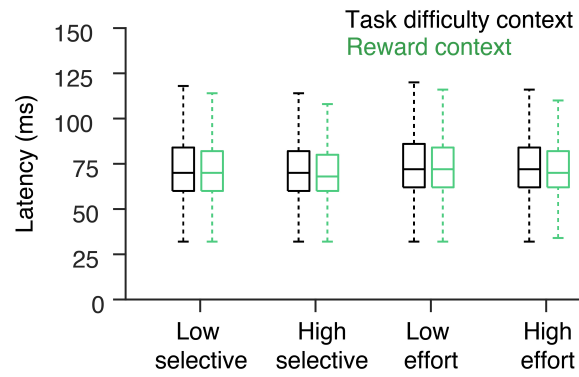


Fig. S14. Latencies to half peak spike response across attention conditions and task contexts of all units. Individual box plots show medians, quartiles and ranges of spike rate latencies for all units in difficulty context ($n = 1134$) and reward context ($n = 1246$) (Materials and Methods). There was no significant difference between the two contextual manipulations ($p = 0.16$, ANOVA; Materials and Methods).

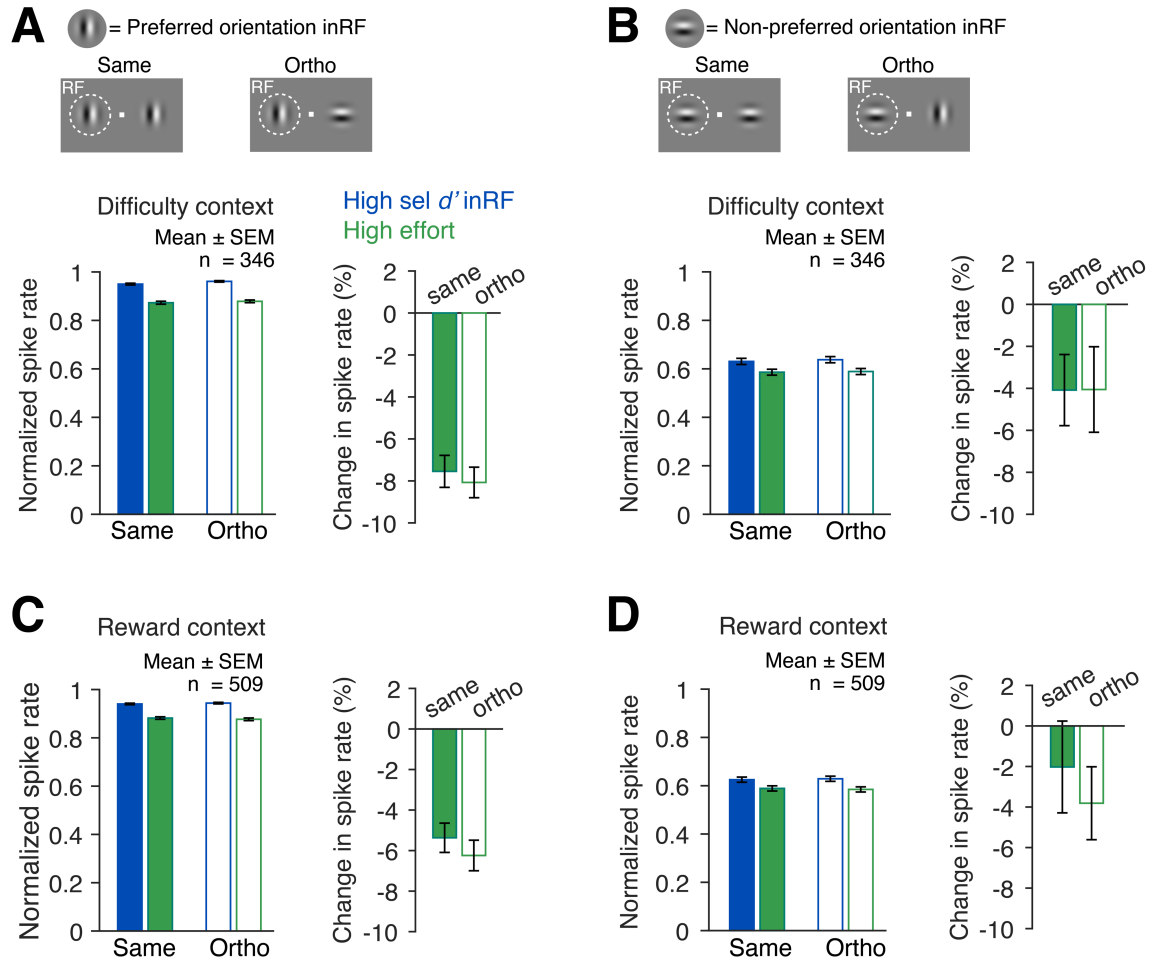


Fig. S15. Comparing attentional modulations for high selective attention and high effort as a function of neurons' orientation selectivity in reference to sample stimuli orientations. (A, C) *Left*, Normalized population average of spike rates for subsets of neurons and trials when neuron's preferred orientation was same as the sample stimulus in the RF location during the task-difficulty sessions (A) and reward manipulation session (C). *Right*, change in spike rates as animals' attention shifts from high selective attention inRF to high effort. Trials were first classified into two groups according to the orientation similarity between sample stimuli in the two locations (inRF and oppRF): same ($|\theta_{\text{inRF}} - \theta_{\text{oppRF}}| < 15^\circ$) and orthogonal ($|\theta_{\text{inRF}} - \theta_{\text{oppRF}}| > 75^\circ$). These groups were further classified according to whether the orientation of inRF sample stimulus matched with the neuron's preferred orientation ($|\theta_{\text{inRF}} - \phi_{\text{prefOri}}| < 15^\circ$) or non-preferred orientation ($|\theta_{\text{inRF}} - \phi_{\text{nonprefOri}}| < 15^\circ$). Where, θ_{inRF} and θ_{oppRF} are respectively sample orientations in the RF and the opposite RF locations; ϕ_{prefOri} and $\phi_{\text{nonprefOri}}$ are respectively neuron's preferred and non-preferred orientations. Error bars, \pm SEM. (B, D) Same as in (A) and (C), but for the trials when neuron's non-preferred orientation was same as the sample stimulus in the RF location during the task-difficulty sessions (B) and reward manipulation session (D).

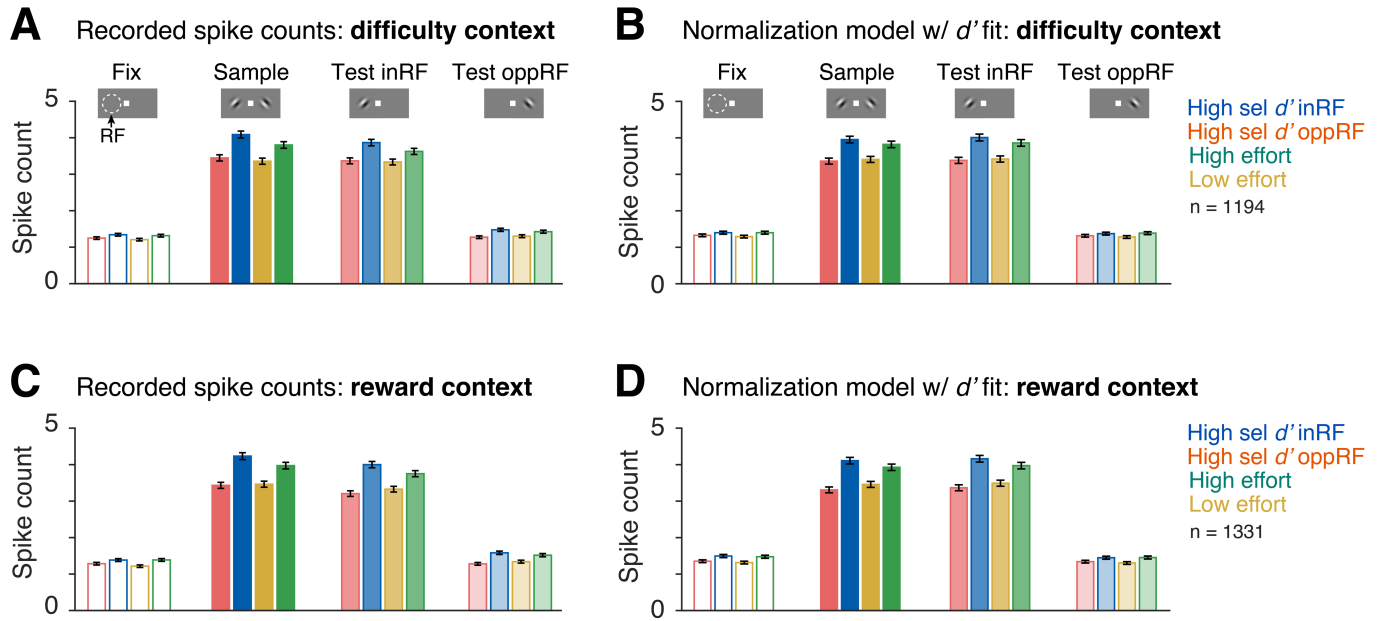


Fig. S16. Comparing observed and normalization model fitted population averaged spike counts across different stimulus and attention conditions. (A) Observed population averaged spike counts over 200 ms during pre-sample (−200 to 0 ms), sample stimuli (60 to 260 ms) and test stimulus (60 to 260 ms) periods for four selective and non-selective attention conditions in task-difficulty sessions ($n = 1194$). (B) Same as in (A) for normalization model (model w/ d') fitted spike counts. (C, D) Same as in (A) and (B), but for varying reward sessions ($n = 1331$), observed (C) and model fitted (D) spike counts.

Data S1 (external): The *.xlsx (Excel) file contains data used in the Figs. 1-6 in the manuscript.

Data S2 (external): The *.mat (Matlab) contains file raw data of PSTHs, spatial receptive fields, neuronal d's of all units in reward context sessions.

Data S3 (external): The *.mat (Matlab) contains raw data of PSTHs, spatial receptive fields, neuronal d's of all units in task difficulty context sessions.